Bioorganic & Medicinal Chemistry Letters 20 (2010) 1293–1297

Contents lists available at ScienceDirect

Bioorganic & Medicinal Chemistry Letters

journal homepage: www.elsevier.com/locate/bmcl

Novel 3-aminopyrazole inhibitors of MK-2 discovered by scaffold hopping strategy

Juraj Velcicky *, Roland Feifel, Stuart Hawtin, Richard Heng, Christine Huppertz, Guido Koch, Markus Kroemer, Henrik Moebitz, Laszlo Revesz, Clemens Scheufler, Achim Schlapbach

Novartis Institutes for BioMedical Research, CH-4002 Basel, Switzerland

ARTICLE INFO

Article history:
Received 22 September 2009
Revised 29 October 2009
Accepted 30 October 2009
Available online 3 November 2009

Keywords:
MK2
TNFα-inhibition
3-Aminopyrazole
Scaffold hopping
Induced-fit
X-ray

ABSTRACT

New, selective 3-aminopyrazole based MK2-inhibitors were discovered by scaffold hopping strategy. The new derivatives proved to inhibit intracellular phosphorylation of hsp27 as well as LPS-induced TNFα release in cells. In addition, selected derivative **14e** also inhibited LPS-induced TNFα release in vivo.

Successful use of *anti*-TNFα biologics etanercept (Enbrel®), infliximab (Remicade®) and adalimumab (Humira®) in the clinic demonstrates a key-role of this cytokine in triggering and sustaining the inflammation in autoimmune diseases such as rheumatoid arthritis, psoriasis, Crohn's disease and others.[1] TNFα is mainly produced by macrophages and its biosynthesis is initiated upon extracellular activation (e.g., LPS) of signaling pathways leading to activation of mitogen-activated protein kinases (MAPKs) such as p38 MAPK (p38).[2] Some time ago, it was shown that MAPKAP kinase-2 (MK2),[3] a direct downstream substrate of p38, plays a crucial role in the signaling and synthesis of TNFα. Evidence using MK2 *k.o.* mice showed decreased TNFα levels in vivo and ex vivo upon LPS stimulation.[3a] Furthermore, these mice were also resistant to collagen-induced arthritis.[4] As MK2 is downstream of p38, less side effects are predicted for MK2 inhibitors compared to p38, whilst retaining the beneficial properties, that is, prevention and treatment of diseases mediated by TNFα. This anticipation led various groups to the search for potent MK2 inhibitors.[5] Recently, we reported our initial chemical efforts in targeting this kinase[5a] and in this study we wish to disclose our strategy towards further modification leading to aminopyrazole series.

In order to substantially modify the pyrrolo-pyrimidinone structure of **1** we employed a scaffold hopping strategy[6] (Fig. 1). Using this approach, we aimed to replace the five-membered pyrrole ring of **1** with a six-membered phenyl ring. In order to fit the new structure (distance and geometry) into the MK2-pharmacophore, the six-membered pyridine ring in **1** had to be substituted with a five-membered heterocycle. General structure of such a new scaffold is represented by a formula **2**.

By screening for a suitable five-membered heterocycle, we have found that pyrazole represented by compound **3b** fitted best to such an exercise (Table 1). Although a simple pyrazole only weakly inhibits MK2 kinase activity, an additional amino group in the 3-position of pyrazole-ring (**3b**) gained potency at MK2 by one log unit (**3b** vs **3a**). An amino group in 5-position of pyrazole (**3c**) led to decreased inhibition of MK2, indicating that the 3-aminopyrazole ring is well positioned for binding to this kinase.

Pyrazole **3a** was prepared in four steps starting with an acidic formation of the pyrazole-ring by a condensation of *p*-methoxyphenyl hydrazine with 1,1,3,3-tetramethoxy-propane (Scheme 1).

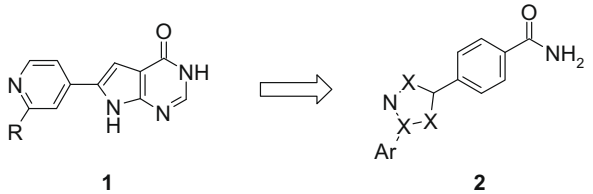

Figure 1. Scaffold hopping strategy in derivatization of scaffold **1**.

* Corresponding author.
E-mail address: juraj.velcicky@novartis.com (J. Velcicky).

0960-894X/$ - see front matter © 2009 Elsevier Ltd. All rights reserved.
doi:10.1016/j.bmcl.2009.10.138

Table 1
Modification of five-membered heterocycle

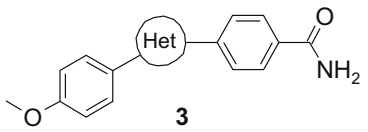

3

Compound	Het	MK2[a] (μM)
1a	R in 1: *p*-MeO-Ph	0.54 ± 0.09
3a		22.6 ± 7.4
3b	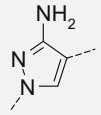	2.0 ± 0.4
3c	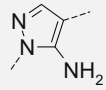	22.5 ± 1.5

[a] Inhibition of kinase activity (IC_{50} values) were measured using a FRET based assay[10] and are reported as a mean of ⩾2 measurements.

Following bromination, Suzuki reaction with *p*-cyanophenyl-boronic acid and hydrolysis of the nitrile led to an amide **3a**. Unfortunately, the synthetic precursor **6a** for preparation of the more potent 3-aminopyrazole **3b** was obtained only as a minor product (**6a**/**6b** = 1:15) under acidic cyclization[7] of the hydrazine with enol **5a**. However, cyclization of the hydrazine with methyl ether **5b** under basic conditions,[8] completely reverts the regioselectivity of this reaction and 3-aminopyrazole intermediate **6a** could be obtained in excellent yield (93%) as a single isomer.

We next aimed to improve the MK2 binding affinity of the 3-aminopyrazole scaffold. Since initial derivatization of *N*-aryl substituent proved to be unsuccessful, we focused on the benzamide portion.

For this purpose, diverse lactames were prepared (Scheme 2) by Suzuki coupling of 3-amino-4-bromopyrazole **9** (reached in two steps by basic condensation of *p*-MeO-phenyl hydrazine with 3-methoxyacrylonitrile followed by NBS bromination) and boronic esters **11a–d** (obtained by palladium catalyzed boronation of the corresponding bromides or triflates known in the literature).[9] Sulfonamide **7** was obtained by Suzuki coupling of bromopyrazole **9** with commercially available 4-sulfamoyl-phenylboronic ester.

Interestingly, while nitrile **6a** and sulfonamide **7** are weaker MK2-inhibitors than amide **3b** (Table 2), freezing the rotation of the amide group by its transformation to a lactame such as **8b** significantly improved the potency at MK2 (IC_{50} of **3b**/**8b** ~25). Quite surprisingly, the lactame ring size was found to be of great importance for this scaffold. While ω-lactames **8c** and **8d** show a drop in the potency (**8c** being in a range of the amide **3b**), γ-lactame **8a** is even less tolerated than the primary amide **3b** (Table 2). Unfortunately, none of the inhibitors described above showed any effect in our cellular assays (inhibition of TNFα11 release in human PBMC cells or phosphorylation of hsp27[12] (p-hsp27) in the monocytic cell line THP-1). This did not appear to be due to the lack of cell penetration as compounds showed reasonable permeability (e.g., **8b:** PAMPA (log Pe pH 6.8: −4.4); Caco-2 (Papp(A − B): 48.3×10^{-6} cm s^{-1}; P(B − A)/P(A−B): 0.31)).

In the search for compounds with cellular potency, we have found that *m*-phenol **14a** shows potency in both cellular assays (TNFα and p-hsp27). Therefore, we explored this further by searching for its biomimetics[13] with less potential to fast in vivo clearance (Table 3).

Since the corresponding anisole derivative **14b** is inactive in the p-hsp27 assay, the hydrogen donor of the phenol seems to be important for cellular activity. This observation was further supported by sulfonamide **14c**, benzimidazole **14d** or indole **14e**, latter being the best compound obtained in terms of MK2 activity as well as cellular potency (Table 3). *N*-Methylation of indole (**14e**) resulted in a cellulary inactive compound **14f**. Interestingly, the 2-indolone compound **14g** (having a hydrogen donor) was inactive for p-hsp27 (>30 μM) as well, indicating that the carbonyl group may negatively interfere with the enzyme (MK2: 0.22 μM).

An insight into the binding of such compounds was obtained by X-ray crystallography of **14e** with MK2 (47–364)[14] (Fig. 2). As expected, the aminopyrazole binds to the hinge region of MK2,

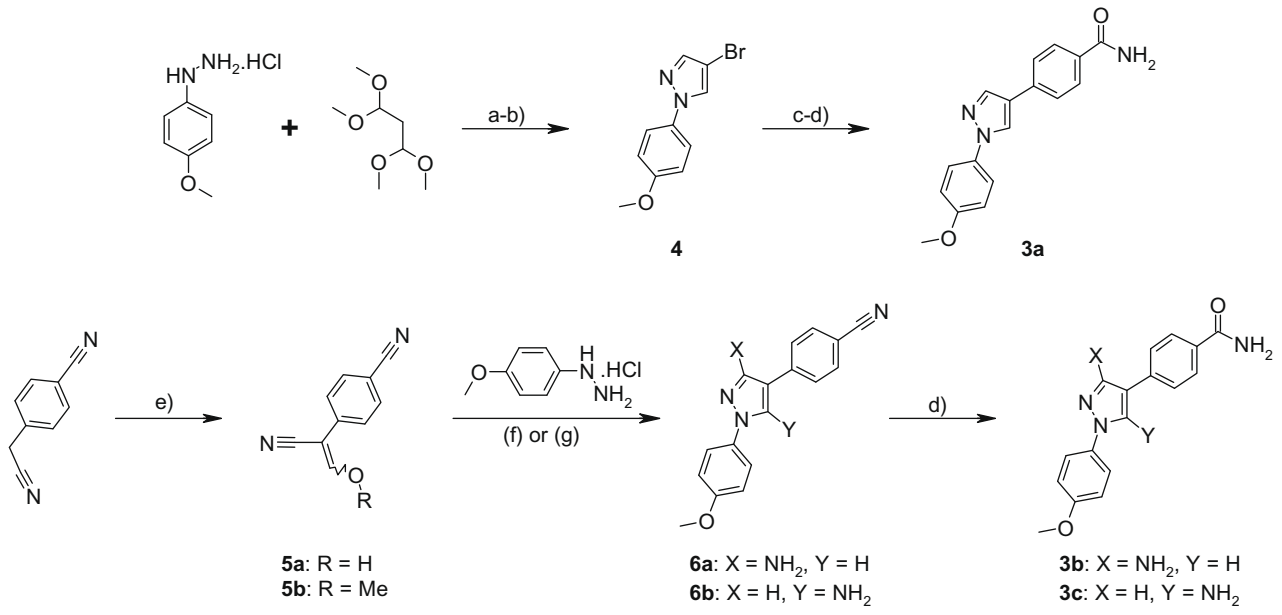

Scheme 1. Reagents and conditions: (a) EtOH, reflux, 1 h (95%); (b) NBS, THF, 23 °C, 3.5 h (95%); (c) *p*-CN-Ph-B(OH)$_2$, $PdCl_2(PPh_3)_2$ (cat.), Na_2CO_3, *n*-PrOH/H_2O; 160 °C, 15 min, microwave (50%); (d) H_2O_2, NaOH, H_2O/MeOH/DMF, 23 °C, 16h (**3a**: 70%; **3b**: 56%; **3c**: 90%); (e) HCOOEt, for **5a**: NaH, DME, 60 °C, 3h (96%); for **5b**: NaOEt, EtOH, 50 °C, 3h, *then* MeI, DMF, 40 °C, 2h (86%); (f) **5a**, EtOH, AcOH, reflux, 3h (**6a**: 3%, **6b**: 46%); (g) **5b**, NaOEt/EtOH, reflux, 4h (**6a**: 93%).

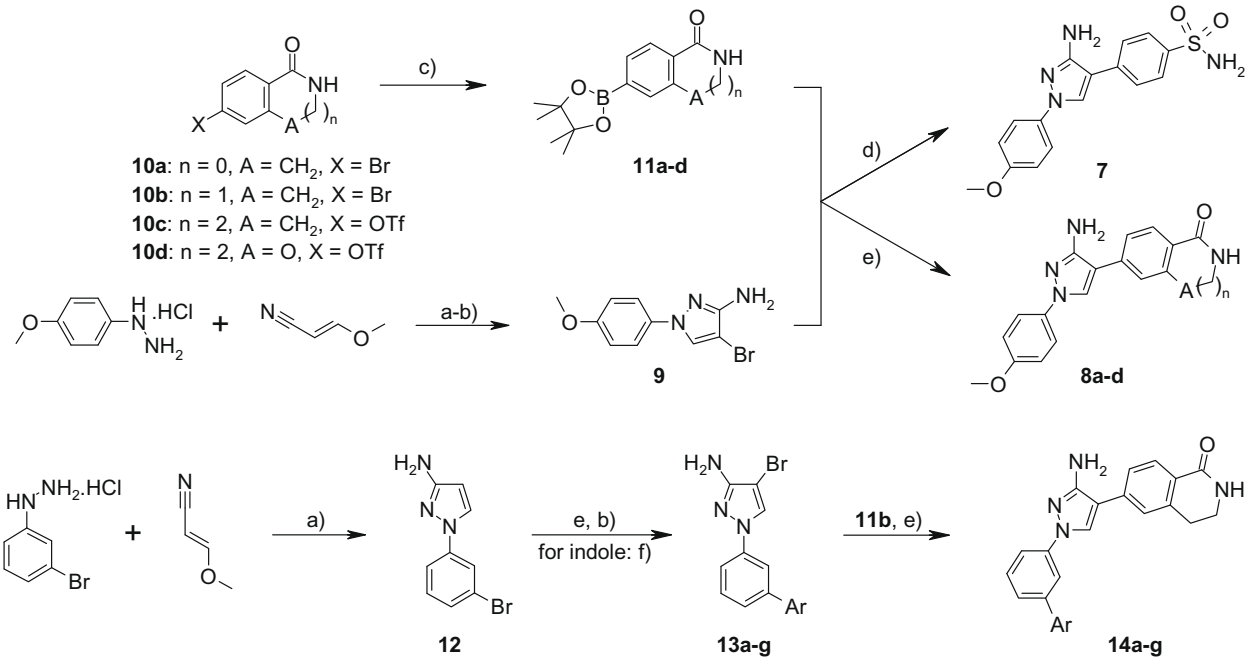

Scheme 2. Reagents and conditions: (a) NaOEt, EtOH, reflux, 20 h (**9**: 73%; **12**: 91%); (b) NBS, THF, 23 °C, 16 h (**9**: 87%; **13a–g**: 51–96% over two steps); (c) pinacolatodiboron, $Pd(dppf)Cl_2$/dppf (cat.), KOAc, dioxane, 80 °C, 16 h (87–97%); (d) 4-boronobenzenesulfonamide pinacol ester, $PdCl_2(PPh_3)_2$ (cat.), Na_2CO_3, *n*-PrOH/H_2O, 150 °C, 15 min, microwave (29%); (e) $PdCl_2(PPh_3)_2$ (cat.), Na_2CO_3, *n*-PrOH/H_2O; 150 °C, 15 min, microwave or for **11b**:80 °C, 16 h (**8a–d**: 17–63%; **14a–g**: 9–36%); (f) NaH, Boc_2O, DMF, rt, 16h (99%).

Table 2
Modification of the amide portion

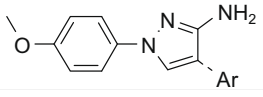

Compound	Ar	MK2[a] (μM)
3b	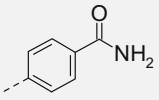	1.98 ± 0.37
6a	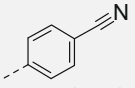	31.2 ± 1.2
7	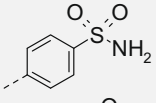	15.4 ± 0.6
8a	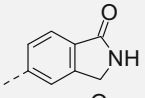	6.0 ± 1.0
8b	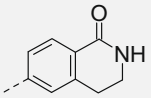	0.084 ± 0.029
8c	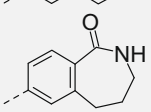	1.1 ± 0.4
8d	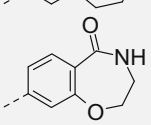	0.35 ± 0.22

[a] IC_{50} values are measured using FRET kinase assay[10] and are reported as a mean of ⩾2 measurements.

Table 3
Search for *m*-phenol biomimetics

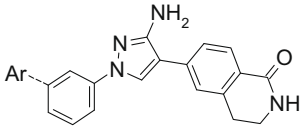

Compound	Ar	MK2[a] (μM)	TNFα[b] (μM)	p-hsp27[c] (μM)
14a	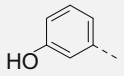	0.18 ± 0.02	2.8 ± 0.7	3.5 ± 1.0
14b	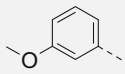	0.18 ± 0.01	4.5 ± 0.4	>30
14c	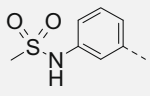	0.18 ± 0.07	>10	⩾11.3
14d	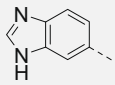	0.082 ± 0.042	5.3 ± 0.9	4.1 ± 0.3
14e	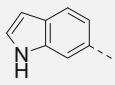	0.061 ± 0.006	2.5 ± 0.8	2.0 ± 0.8
14f	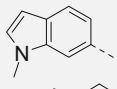	0.29 ± 0.07	>10	>30
14g	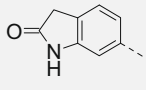	0.22 ± 0.12	⩾3.8	>30

[a] IC_{50} values are measured using FRET kinase assay[10] and are reported as a mean of ⩾2 measurements.
[b] Inhibition of LPS stimulated release of TNFα from human PBMCs.[11]
[c] Inhibition of anisomycin stimulated phosphorylation of hsp27 in THP-1 cells.[12]

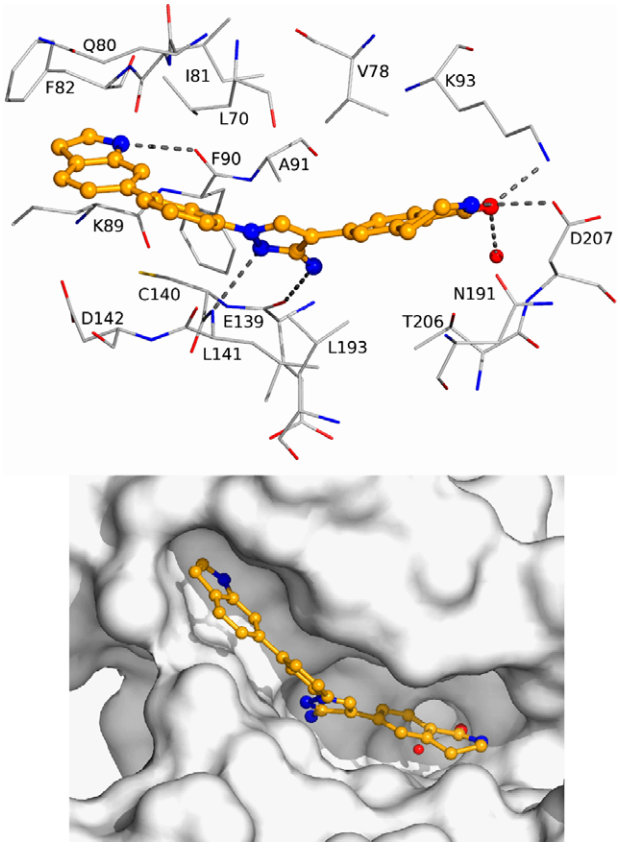

Figure 2. Crystal structure of **14e** bound to MK2.[14]

interacting with backbone of E139 and L141, and the lactame portion makes a dual hydrogen bond interaction with residues of conserved K93 and D207. Surprisingly, an unusual binding of the indole-ring to a new, ligand induced hydrophobic pocket behind MK2-hinge region was observed. The indole-NH group forms an additional hydrogen bond interaction with the backbone carbonyl of F90, highlighting the importance of an hydrogen donor at this position. The induced-fit of MK2 with compound **14e** most probably favors the observed high selectivity (IC_{50} >10 μM) of this inhibitor against 29 different kinases in our *in house* kinase panel including CDK2, JNK1, JNK2 and p38α as well as its low toxicity in THP-1 cell proliferation assay (IC_{50} >20 μM).

In addition, compound **14e** also inhibited LPS-induced TNFα release in mice.[15] Although good inhibition (68%) was observed at 100 mg/kg po dosage (blood levels of 17.4 μM), no inhibition was observed at a lower 30 mg/kg po dose. This was not surprising as the blood levels at the lower dose (1.7 μM) did not reach levels expected to exert an effect as demonstrated using human PBMCs. One possible explanation for the lack of linearity in the dose/blood levels could be due to the low solubility of this compound (<2 mg/L at pH 1, 4 and 6.8). In an additional study, a concentration dependant effect was observed when TNFα levels were measured at different time points after compound dosing. Thus, dosing the compound 1 h before LPS challenge yields in 66% inhibition at 14.1 μM blood exposure; 4 h before LPS challenge (23% at 6.8 μM) and 6 h (67% at 25.8 μM). This study also indicates a second absorption peak at 4–6 h, which may be caused by the low solubility of this compound. Therefore, we are currently further searching for more potent and more soluble analogs of **14e**.

In a summary, we have discovered and profiled novel 3-aminopyrazole MK2-inhibitors. This new class was revealed by scaffold hopping strategy and could be developed to obtain a selective MK2 kinase inhibitor **14e**. This compound showed potent inhibition of MK2 activity and reasonable cellular activity (inhibition of TNFα and phoshorylation of hsp27). In addition, the compound was effective in vivo for inhibition of LPS-induced TNFα release in mice. Interestingly, a novel binding pocket behind the hinge region which was induced by the ligand was discovered which seems to improve binding to MK2 and also kinase selectivity.

Acknowledgments

We are very grateful to our colleagues from the NIBR kinase platform for providing us with in vitro kinase and selectivity data as well as the NIBR Prep Labs for the syntheses of valuable intermediates.

References and notes

1. (a) Feldmann, M.; Maini, R. N. *Nat. Med.* **2003**, *9*, 1245; (b) Nikolaus, S.; Schreiber, S. *Der Internist* **2008**, *49*, 947; (c) Valesini, G.; Iannuccelli, C.; Marocchi, E.; Pascoli, L.; Scalzi, V.; Di Franco, M. *Autoimmunity Rev.* **2007**, *7*, 35; (d) Mousa, S. A.; Goncharuk, O.; Miller, D. *Expert Opin. Biol. Ther.* **2007**, *7*, 617; (e) Takeuchi, T.; Amano, K.; Kameda, H.; Abe, T. *Allergol. Int.* **2005**, *54*, 191.
2. (a) Schindler, J. F.; Monahan, J. B.; Smith, W. G. *J. Dent. Res.* **2007**, *86*, 800; (b) Peifer, C.; Wagner, G.; Laufer, S. *Curr. Top. Med. Chem.* **2006**, *6*, 113; (c) Dominguez, C.; Powers, D. A.; Tamayo, N. *Curr. Opin. Drug Disc. Dev.* **2005**, *8*, 421.
3. (a) Kotlyarov, A.; Neininger, A.; Schubert, C.; Eckert, R.; Birchmeier, C.; Volk, H.-D.; Gaestel, M. *Nat. Cell Biol.* **1999**, *1*, 94; (b) Kotlyarov, A.; Yannoni, Y.; Fritz, S.; Laaß, K.; Telliez, J.-B.; Pitman, D.; Lin, L.-L.; Gaestel, M. *Mol. Cell. Biol.* **2002**, *22*, 4827; (c) Neininger, A.; Kontoyiannis, D.; Kotlyarov, A.; Winzen, R.; Eckert, R.; Volk, H.-D.; Holtmann, H.; Kollias, G.; Gaestel, M. *J. Biol. Chem.* **2002**, *277*, 3065; (d) Duraisamy, S.; Bajpai, M.; Bughani, U.; Dastidar, S. G.; Ray, A.; Chopra, P. *Expert Opin. Ther. Targets* **2008**, *12*, 921.
4. Hegen, M.; Gaestel, M.; Nickerson-Nutter, C. L.; Lin, L. L.; Telliez, J. B. *J. Immunol.* **2006**, *177*, 1913.
5. (a) Schlapbach, A.; Feifel, R.; Hawtin, S.; Heng, R.; Koch, G.; Moebitz, H.; Revesz, L.; Scheufler, C.; Velcicky, J.; Waelchli, R.; Huppertz, C. *Bioorg. Med. Chem. Lett.* **2008**, *18*, 6142; (b) Anderson, D. R.; Hegde, S.; Reinhard, E.; Gomez, L.; Vernier, W. F.; Lee, L.; Liu, S.; Sambandam, A.; Snider, P. A.; Masih, L. *Bioorg. Med. Chem. Lett.* **2005**, *15*, 1587; (c) Wu, J.-P.; Wang, J.; Abeywardane, A.; Andersen, D.; Emmanuel, M.; Gautschi, E.; Goldberg, D. R.; Kashem, M. A.; Lukas, S.; Mao, W.; Martin, L.; Morwick, T.; Moss, N.; Pargellis, C.; Patel, U. R.; Patnaude, L.; Peet, G. W.; Skow, D.; Snow, R. J.; Ward, Y.; Werneburg, B.; White, A. *Bioorg. Med. Chem. Lett.* **2007**, *17*, 4664; (d) Trujillo, J. I.; Meyers, M. J.; Anderson, D. R.; Hegde, S.; Mahoney, M. W.; Vernier, W. F.; Buchler, I. P.; Wu, K. K.; Yang, S.; Hartmann, S. J.; Reitz, D. B. *Bioorg. Med. Chem. Lett.* **2007**, *17*, 4657; (e) Goldberg, D. R.; Choi, Y.; Cogan, D.; Corson, M.; DeLeon, R.; Gao, A.; Gruenbaum, L.; Hao, M. H.; Joseph, D.; Kashem, M. A.; Miller, C.; Moss, N.; Netherton, M. R.; Pargellis, C. P.; Pelletier, J.; Sellati, R.; Skow, D.; Torcellini, C.; Tseng, Y.-C.; Wang, J.; Wasti, R.; Werneburg, B.; Wu, J. P.; Xiong, Z. *Bioorg. Med. Chem. Lett.* **2008**, *18*, 938; (f) Xiong, Z.; Gao, D. A.; Cogan, D. A.; Goldberg, D. R.; Hao, M.-H.; Moss, N.; Pack, E.; Pargellis, C.; Skow, D.; Trieselmann, T.; Werneburg, B.; White, A. *Bioorg. Med. Chem. Lett.* **2008**, *18*, 1994; (g) Anderson, D. R.; Meyers, M. J.; Vernier, W. F.; Mahoney, M. W.; Kurumbail, R. G.; Caspers, N.; Poda, G. I.; Schindler, J. F.; Reitz, D. B.; Mourey, R. J. *J. Med. Chem.* **2007**, *50*, 2647; (h) Lin, S.; Lombardo, M.; Malkani, S.; Hale, J. J.; Mills, S. G.; Chapman, K.; Thompson, J. E.; Zhang, W. X.; Wang, R.; Cubbon, R. M.; O'Neill, E. A.; Luell, S.; Carballo-Jane, E.; Yang, L. *Bioorg. Med. Chem. Lett.* **2009**, *19*, 3238; i Anderson, D. R.; Meyers, M. J.; Kurumbail, R. G.; Caspers, N.; Poda, G. I.; Long, S. A.; Pierce, B. S.; Mahoney, M. W.; Mourey, R. J. *Bioorg. Med. Chem. Lett.* **2009**, *19*, 4878; j Anderson, D. R.; Meyers, M. J.; Kurumbail, R. G.; Caspers, N.; Poda, G. I.; Long, S. A.; Pierce, B. S.; Mahoney, M. W.; Mourey, R. J.; Parikh, M. D. *Bioorg. Med. Chem. Lett.* **2009**, *19*, 4882.
6. (a) Schneider, G.; Neidhart, W.; Giller, T.; Schmid, G. *Angew. Chem., Int. Ed.* **1999**, *38*, 2894; (b) Schneider, G.; Schneider, P.; Renner, S. *QSAR Comb. Sci.* **2006**, *25*, 1162; (c) Böhm, H.-J.; Flohr, A.; Stahl, M. *Drug Discovery Today* **2004**, *1*, 217; see also: (d) Mauser, H.; Guba, W. *Curr. Opin. Drug Disc. Dev.* **2008**, *11*, 365; (e) Zhao, H. *Drug Discovery Today* **2007**, *12*, 149.
7. (a) Silvestri, R.; Cascio, M. G.; La Regina, G.; Piscitelli, F.; Lavecchia, A.; Brizzi, A.; Pasquini, S.; Botta, M.; Novellino, E.; Di Marzo, V.; Corelli, F. *J. Med. Chem.* **2008**, *51*, 1560; (b) Harvey, A. L.; MacTavish, J.; Mullins, S. J.; Proctor, G. R. *J. Chem. Res., Synop.* **1997**, *11*, 420.
8. Iida, T.; Satoh, H.; Maeda, K.; Yamamoto, Y.; Asakawa, K.; Sawada, N.; Wada, T.; Kadowaki, C.; Itoh, T.; Mase, T.; Weissman, S. A.; Tschaen, D.; Krska, S.; Volante, R. P. *J. Org. Chem.* **2005**, *70*, 9222.
9. a γ-lactame-bromide: Clayton, J.; Ma, F.; Van Wagenen, B.; Ukkiramapandian, R.; Egle, I.; Empfield, J.; Isaac, M.; Slassi, A.; Steelman, G.; Urbanek, R.; Walsh, S. WO 2006/020879.; b δ-lactame-bromide: Coppola, G. M.; Damon, R. E.; Kukkola, P. J.; Stanton, J. L. WO 2004/065351.; ω-lactame-triflates were obtained by triflation (**11c**: Tf_2O, Et_3N, DMAP (cat.), CH_2Cl_2, −78 °C to 23 °C,

18 h, 67%; **11d**: Tf_2O, pyridine, 23 °C, 18 h, 35%) of the literature known phenols: (c) Shtacher, G.; Erez, M.; Cohen, S. *J. Med. Chem.* **1973**, *16*, 516.

10. MK2 was pre-activated in kinase buffer (25 mM Tris–HCl, pH 7.5, 25 mM β-glycerophosphate, 0.1 mM Na_3VO_4, 25 mM $MgCl_2$, 20 μM DTT) containing 5 μM ATP, 150 μg/ml human MK2, 30 μg/ml active human p38α for 30 min at 22 °C. For MK2 inhibition, reactions contained compound (10 μl; 0.5% DMSO final) or vehicle control, 250 nM hsp27 peptide biotinyl-AYSRALSRQLSSGVSEIR-COOH as substrate (10 μl) and activated MK2 mix (10 μl) containing ATP (5 μM final). Following incubation at 22 °C for 45 min, reactions were terminated with 125 μM EDTA (10 μl). Samples (10 μl) were transferred to black 384-well plates for detection of p-hsp27 by time-resolved fluorescence resonance energy transfer using an antibody mix (10 μl) containing a rabbit anti-phospho-hsp27 (Ser^{82}) antibody (2.5 M, Upstate), and anti-rabbit europium-labeled secondary antibody LANCE Eu-W1024 (3.6 nM; Perkin Elmer) as fluorescence donor along with streptavidin SureLight-APC (6.25 nM; Perkin Elmer) as acceptor. Following incubation at 22 °C for 90 min, the FRET ratio 665/620 nm was determined.
11. Human peripheral blood mononuclear cells (hPBMCs) were prepared from peripheral blood of healthy volunteers using Ficoll-Plaque Plus (Amersham) density separation. Cells were seeded at a 1×10^5 cells/well in 96-well plates in RPMI 1640 medium (Invitrogen) containing 10% (v/v) fetal calf serum. After pre-incubation with serial dilutions of test compound (0.25% v/v DMSO final) for 30 min at 37 °C, cells were stimulated with the addition of IFNγ (10 ng/ml) and lipopolysaccharide (LPS) (5 μg/ml) per well and incubated for 3 h at 37 °C. Following a brief centrifugation, supernatant (10 μl) sample from each well was quantified against TNFα calibration curve using HTRF TNFα kit (CisBio).
12. THP-1 cells were stimulated with anisomycin (25 μl) diluted in low-serum RPMI media (150 ng/ml final) for 15 min at 37 °C. Following stimulation, cells were fixed with 10% (w/v) paraformaldehyde (34 μl; 1.8% v/v final), briefly mixed and incubated for 10 min at 37 °C. Plates were briefly centrifuged (720 g for 5 min at 4 °C) prior to careful aspiration of media on ice. Cells were permeabilised with the addition of 1 ml ice-cold 90% (v/v) methanol, centrifuged (720g for 5 min at room temperature) following the addition of wash buffer (0.5 ml) (PBS containing 1% v/v FCS). Cells were washed twice (1.5 ml) with careful aspiration of media and repeated centrifugation steps. The primary antibody anti-phospho (Ser^{78}) hsp27 diluted to 1:125 in wash buffer (25 μl/well) was incubated on cells for 60 min at room temperature. Cells were washed, prior to incubation with secondary goat anti-rabbit IgG ALEXA (fluor) 647-conjugated antibody diluted 1:5000 in wash buffer (50 μl/well) for 60 min at room temperature in the dark. Cells were washed as described above, prior to careful resuspension in wash buffer (50 μl) for FACS (fluorescence activated cell sorting) analysis. Cells were transferred to 'V' bottom 96-well plates and analysed using a FACSCalibur™ cytometer (Becton Dickinson) equipped with red-diode laser (excitation 635 nm). Gating of cells according to forward and side scatter, mean fluorescent intensity (MFI) was calculated at 653–669 nm (emission).
13. (a) Wermuth, C. G.. In *The Practice of Medicinal Chemistry*; Academic Press: London, 2003; Vol. 2; see also: (b) Lima, L. M.; Barreiro, E. J. *Curr. Med. Chem.* **2005**, *12*, 23; (c) Chen, X.; Wang, W. *Ann. Rep. Med. Chem.* **2003**, *38*, 333.
14. X-ray crystal structure was obtained with 2.55 Å resolution. The X-ray coordinates are deposited with RCSB Protein Data Bank, deposition code is 3KGA; The protein used in this study is a segment of MK2 containing residues 47–364Δ(216–237)G.
15. The MK2 compound was administered po to OF1 mice (female, 8 weeks old), followed by LPS injection (20 mg/kg) 1 h later. 1 h post LPS injection the experiment was terminated and blood withdrawn. Compound blood levels were determined by LC–MS/MS and plasma levels of mouse TNFα determined by ELISA.